Lab on a Chip

PAPER

View Article Online
View Journal | View Issue

Cite this: *Lab Chip*, 2023, **23**, 3479

Viral load quantitation at the point-of-care with shaken digital droplet RT-LAMP

Daniel W. Weisgerber,[a] Krzysztof Langer,[a] Venice Servellita,[b] Peng Xu,[a] Charles Y. Chiu[bc] and Adam R. Abate *[ad]

Received 2nd February 2023,
Accepted 20th April 2023

DOI: 10.1039/d3lc00096f

rsc.li/loc

Viral load quantitation is useful in clinical point-of-care settings to assess the status of patients with infectious disease, track response to treatment, and estimate infectiousness. However, existing methods for quantitating viral loads are complex and difficult to integrate into these settings. Here, we describe a simple, instrument-free approach for viral load quantitation suitable for point-of-care use. We develop a shaken digital droplet assay that can quantitate SARS-CoV2 with sensitivity comparable to gold standard qPCR.

Introduction

Disease monitoring at home or in clinical point-of-care (POC) settings provides valuable information for guiding patient behavior and treatment.[1,2] These settings, however, place severe constraints on the testing modality, as the individual conducting the test is typically unskilled and lacks laboratory equipment.[3–5] The primary approaches appropriate for these settings are thus lateral flow assays based on antigen detection or isothermal nucleic acid amplification based on loop-mediated isothermal amplification (LAMP).[6–8] Antigen tests are fast and cheap but have limited sensitivity.[9–11] LAMP tests are sensitive and accurate but, like antigen tests, provide qualitative results.[12–14] Tests that generated quantitative viral load information would be clinically useful in monitoring disease status, evaluating response to treatment, and estimating patient infectiousness.[15,16]

When viral load must be quantitated, the primary strategies are plaque assays and laboratory-based qPCR.[17–19] In addition to providing an estimate of viral load, plaque assays report on virus viability; however, they are laborious and take days to yield a result, negating their utility in POC settings. Alternatively, qPCR is quantitative, fast (<2 h), and sensitive (down to ~1.5 copies per μL or ~100 copies per mL) but requires specialized instrumentation and incorporates steps that are incompatible with POC testing.[20] Moreover, in addition to requiring standard curves for normalization, qPCR is inaccurate at concentrations relevant to many viral infections (<1000 copies per mL),[21,22] such that results must nevertheless be reported as qualitative positive/negative. By contrast, digital droplet PCR (ddPCR) obtains absolute counts of target viruses without requiring standard curves and is more accurate at low concentrations and more reliable in practice; however, ddPCR machines are complex and even more expensive than qPCR machines and, thus, only used in settings that can justify the expense, such as for cancer diagnostics.[23–25] To make viral load quantitation practical in POC settings, a new strategy is needed that obtains accurate, absolute target counts at concentrations relevant to viral infections, and in a form factor appropriate for the constraints of this setting.

In this paper, we describe shaken digital droplet reverse transcription-LAMP (sdd RT-LAMP) for viral load quantitation at the POC. Our approach is analogous to ddPCR in which target molecules are counted *via* optical detection in picoliter droplets. To make this feasible as a POC diagnostic, we replace the RT-PCR with isothermal RT-LAMP and use shaken rather than microfluidic emulsions. Additionally, rather than imaging droplets individually with high resolution microscopy or microfluidic-based laser induced fluorescence, we develop a dual-height imaging chamber that accommodates the full sample in one photograph captured with a cell phone. The dual-height chamber allows accurate target quantitation over three orders-of-magnitude of dynamic range. The result is an entirely instrument-free viral load quantitation assay meeting the constraints of POC testing. To demonstrate this, we use it to analyze 111 patient samples collected at UCSF in 2020–21 during the height of the SARS-CoV-2 Alpha variant wave of the COVID-19 pandemic. This work demonstrates the feasibility of quantitative viral load testing in POC settings using digital nucleic acid quantitation.

[a] *Department of Bioengineering and Therapeutic Sciences, University of California, San Francisco, CA USA. E-mail: adam@abatelab.org*
[b] *Department of Laboratory Medicine, University of California, San Francisco, CA USA*
[c] *Department of Medicine, Division of Infectious Diseases, University of California, San Francisco, CA USA*
[d] *Chan Zuckerberg Biohub, San Francisco, CA USA*

Results and discussion

Quantitative sddRT-LAMP assay for point of care use

For a test to be suitable for point of care use, it must be simple. Thus, we have designed our viral load quantitation test to use no specialized microfluidics or laboratory equipment. The test begins by collecting a sample from the patient (Fig. 1a) and storing it in viral transport medium. The sample can be frozen and biobanked for future analysis or analyzed immediately. To perform the test, the sample is diluted in quick extract buffer and lysed for 5 minutes; then the RT-LAMP reaction mix and encapsulation oil is added (Fig. 1b) and the tube shaken by hand for 30 seconds, generating a polydispersed emulsion (Fig. 1c). The emulsion is heated on a block for 30 minutes at 65 °C during which droplet LAMP occurs. Droplets containing target virus become positively fluorescent while empty ones remain dim. To quantitate the sample, the emulsion must be imaged, which we achieve with an imaging chamber. The chamber has two heights, a shallow region (80 μm) for single-layer imaging and a tall region (190 μm) for multi-layer imaging. To image the sample, we use a fluorescence imaging device built on a smartphone (Fig. 1d). The images are processed to detect and count positive droplets, providing the target concentration.

Shaken emulsion assay for viral load quantitation of SARS-CoV-2

We developed a sddRT-LAMP assay to detect and accurately quantitate SARS-CoV-2 RNA using primers and FAM-labeled probes targeting the nucleoprotein (N) gene of SARS-CoV-2 (Fig. 2a). To perform sddRT-LAMP, the sample and reaction mix were emulsified by hand shaking for ~30 s with surfactant laden oil, generating picoliter droplets, some encapsulating single target molecules. The resultant polydispersed emulsion had an average droplet size of ~15 μm (Fig. 2b, blue). Due to the viscosity and interfacial tension of the reagents, this was deemed to be the minimum size easily achievable by hand shaking and provided ~10 million total droplets for a 20 μL sample. Due to polydispersity and the cubic dependence of droplet volume on diameter, large droplets, albeit rare, were found to engulf a sizable fraction

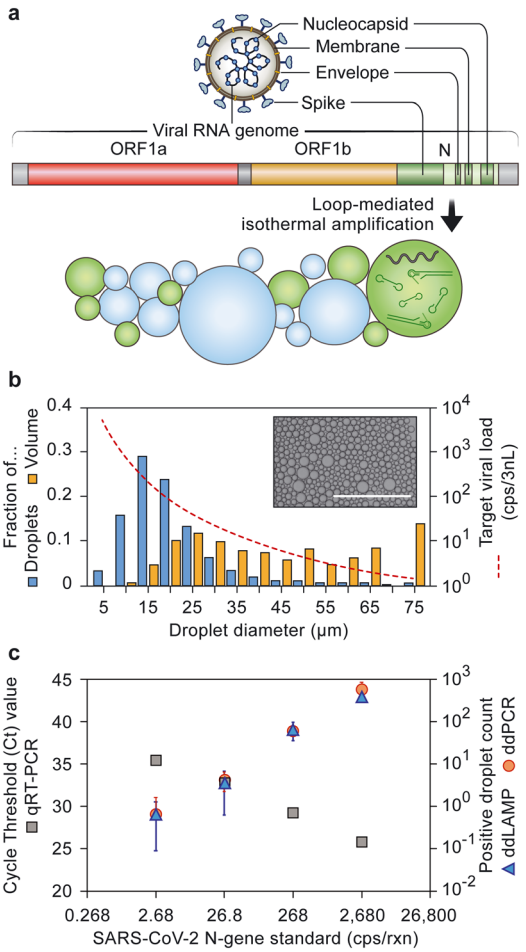

Fig. 2 Characterization of sddLAMP assay. a) SARS-CoV2 genome and locations of LAMP reaction primers. b) Droplet diameter distribution (blue) and corresponding droplet volume fractions (orange). Black line indicates concentration (right axis) to achieve 10% loading of droplet of size determined by *x*-axis. c) Comparison of sddLAMP imaged in a single layer chip with qPCR and ddPCR.

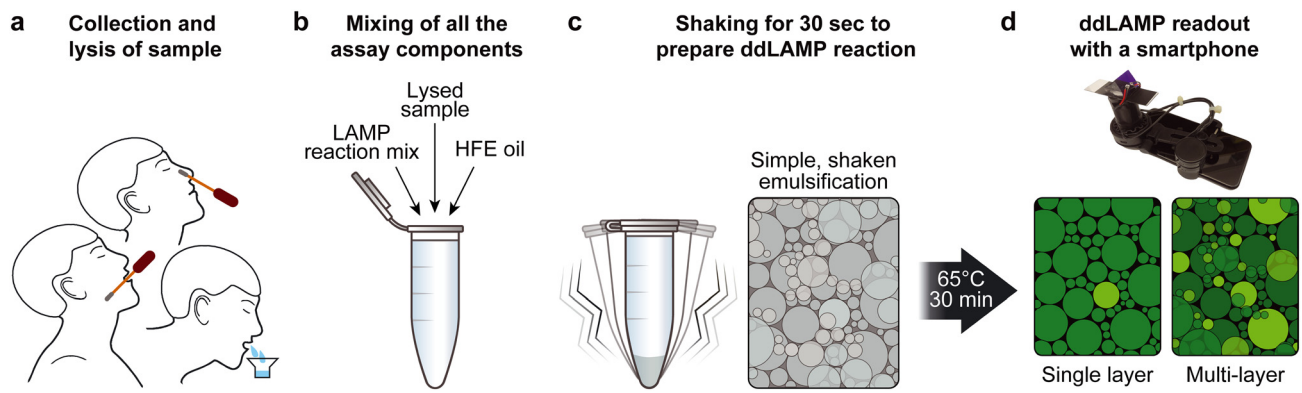

Fig. 1 Microfluidic-free digital droplet test for quantification of viral pathogens. a) Nasal or saliva patient samples are collected and lysed. b) Patient sample and LAMP master mix are combined with emulsification oil. c) Tubes are agitated for 30 s then elevated to 65 °C for 30 minutes. d) Optical detection of digital droplet readout *via* smartphone.

of the sample (Fig. 2b, orange). The inherent polydispersity of the emulsions allowed a range of reactor sizes in a single reaction, as illustrated by the optimal loading rate of 10% for droplets of a given size at different target concentrations (Fig. 2b, red dashed line). Even polydisperse, ≥70% of the sample volume is encapsulated in droplets ≤65 μm in diameter (Fig. 2b, orange bars), allowing an accurate estimation of concentration disregarding sample polydispersity for appropriate sample concentrations (Fig. 2b, red dashed line).

To confirm the efficacy of our assay, we compared sddRT-LAMP to gold standard qPCR testing. We generated a dilution series over a range of concentrations from 2.68 to 2680 copies/reaction (536 to 536 000 copies per mL) and analyzed the samples with both methods, observing good correspondence (Fig. 2c). These results demonstrated that sddRT-LAMP provides quantitation equivalent to gold standard qPCR, but in a form factor practical for POC applications.

Multilayer imaging allows accurate quantitation over a wide dynamic range

To enable accurate target quantitation with droplet counting, we developed an imaging chamber that is easy to load, can accommodate the entire 20 μL sample in a single field of view, and allows accurate droplet quantitation over ~3 orders of magnitude (Fig. 3a). The device consists of a circular chamber with in- and out-ports that draw in emulsified sample by capillary action. To allow complete imaging of the sample, the chamber area and height are designed to accommodate the total sample volume while optimizing for the size and resolution of the camera sensor. For the requisite chamber height to accommodate the full sample, the droplets stack in multiple layers. To allow a portion of the emulsion to be imaged as a monolayer, we thus include a shallow region (80 μm) for a portion of the chamber (Fig. 3b). When virus concentration is low (<10 copies), positive droplets are rare and, thus, tend to be isolated even in the multilayer region, allowing them to be individually counted (Fig. 3c). In contrast, when the target virus concentration is high (>100 cp), positive droplets are prevalent and tend to overlap in the multilayer region, impeding their quantitation; however, the monolayer regions tend to separate the positives in these cases, allowing them to be accurately quantitated (Fig. 3d). Thus, this two-height imaging chamber provides a simple means by which to obtain accurate measurements over a wide range of target concentrations.

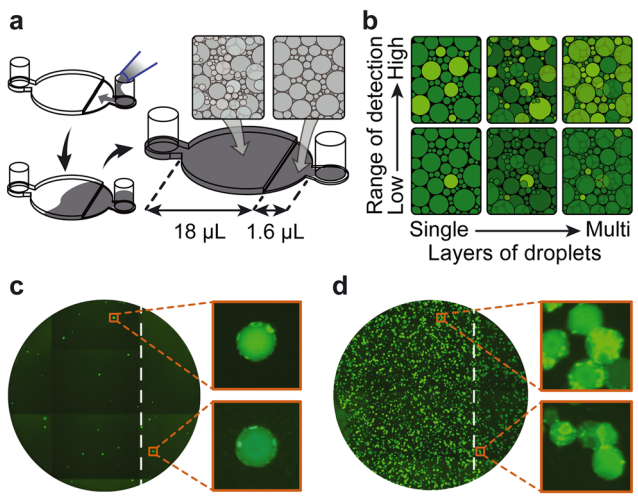

Fig. 3 Dual height imaging chamber for increased dynamical range. a) The imaging chamber is loaded with emulsion through an inlet port, which is drawn in by capillary forces. b) The shallow region allows individual droplet counting under high concentrations (upper-left), and the tall region allows the entire sample to be accommodated while still permitting individual droplet counting under low target concentrations (lower-right). Example fluorescence images of samples with low c) and high d) target concentrations.

Imaging and counting of droplets using a smartphone

Current smartphones have cameras with high sensitivity and resolution and, using inexpensive commercially available hardware, can be used as simple fluorescence microscopes. To illustrate the feasibility of using such a device for droplet quantitation, we designed an optical system that mounts on a smartphone (Fig. 4a). The system consists of a commercially available device with the components needed for epifluorescence microscopy, including a 10× objective lens for high resolution imaging, excitation light sources to induce fluorescence, and battery power. To use the device for droplet counting, the sample chamber is placed on the imaging plate, illumination is activated, and an image captured by the camera (Fig. 4b). A commercial application allows the camera settings to be adjusted to achieve the best picture (Moments by Moment Inc.). To determine the effectiveness of this device, we first analyzed the sample with a laboratory epifluorescence microscope, providing a ground-truth image for droplet quantitation (Fig. 4c). We then imaged the sample with the smartphone (Fig. 4d). The smartphone image was of poorer quality, with a higher light background and overall lower resolution; nevertheless, even under these conditions, positive droplets were visible in both the multi- and mono-layer regions, thus demonstrating feasibility of droplet counting.

Viral load quantitation from clinical SARS-CoV2 samples

To validate our approach for POC settings, we used it to analyze 111 patient samples collected at the University of California, San Francisco (UCSF) Clinical Microbiology Laboratory from 2020–21. Over this time, the Alpha (B.1.1.7) variant was the dominant circulating SARS-CoV-2 variant, and thus specifically targeted by our primers. We analyzed samples with viral titers ranging from 1 to 5000 copies/reaction (200 to 1 000 000 copies per mL) using sddRT-LAMP. Low titers yielded few positive droplets (Fig. 5a) while medium and high titers yielded corresponding proportions of positive droplets (Fig. 5b and c). Our assay was specific, with

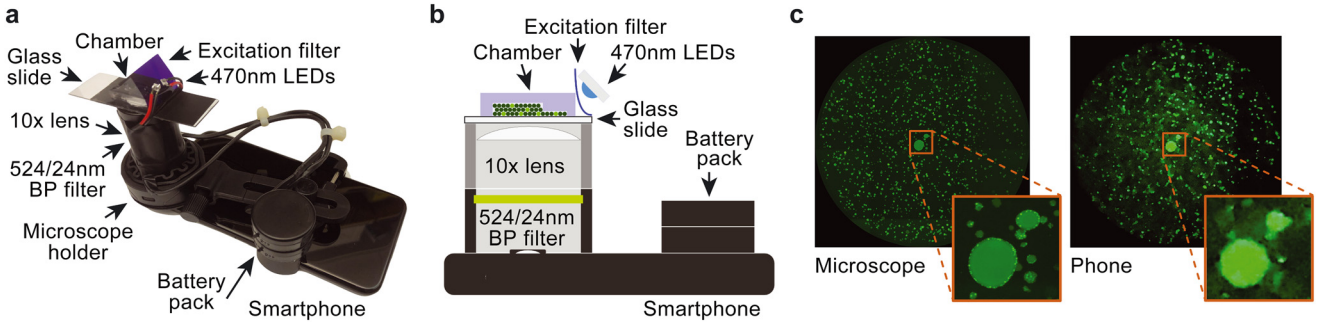

Fig. 4 Smartphone droplet counting device. a) A commercially available smartphone attachment transforms a smartphone into a low-cost fluorescence microscope. b) The sample is imaged by placing it on the imaging mount. Comparison of c) laboratory microscope and smartphone imaging of the same sddLAMP sample.

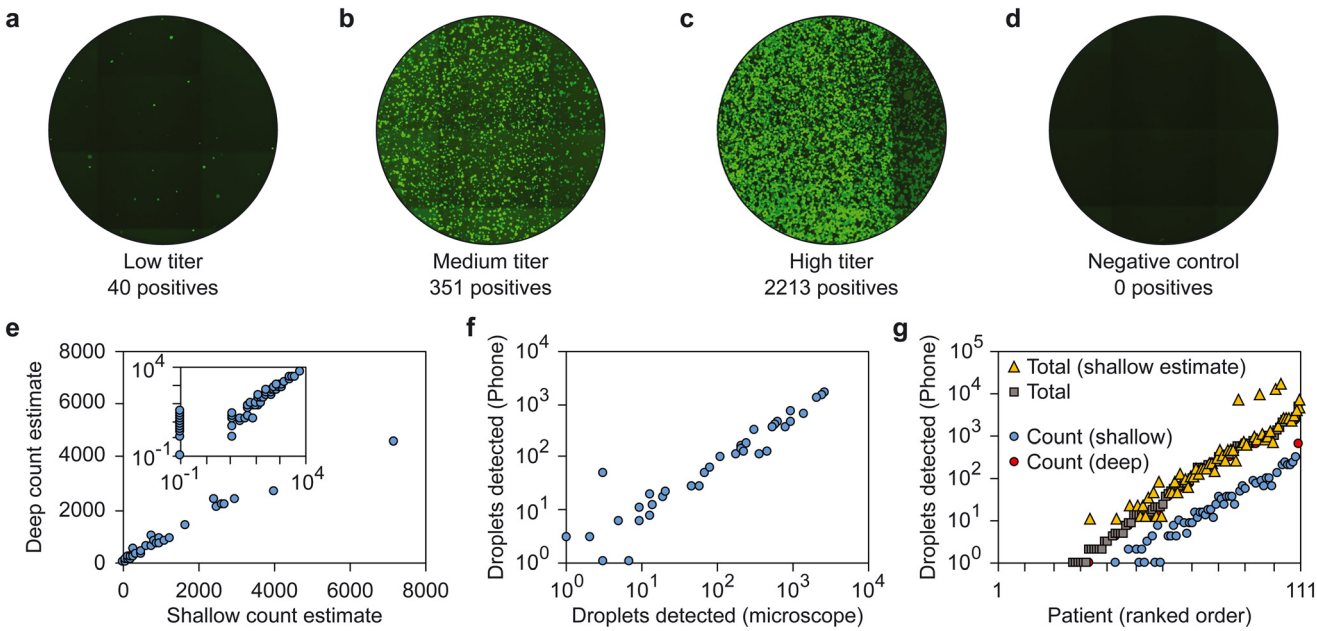

Fig. 5 Evaluation of 111 patient samples with sddRT-LAMP. Example images of sddRT-LAMP samples from patients with a) low, b) medium, and c) high viral loads. d) Negative control showing no off-target amplification. e) Concentration estimates from short (*x* axis) and tall (*y* axis) regions from sample chamber. f) Scatter plot of detected droplets with laboratory microscope (*x*-axis) and smartphone (*y*-axis) imaging. Due to its lower resolution and higher light background, the smartphone detects roughly half the positives, though the correlation with the microscope remains high (0.98). g) Droplets detected in the shallow and deep regions with the combined total, and the associated estimate based on the shallow region counts alone.

negative controls showing no positive droplets (Fig. 5d). The short and tall viewing regions correlated strongly and demonstrated the efficacy of dual height imaging for increasing dynamical range (Fig. 5e). The smartphone tended to undercount positive droplets likely due to the lower resolution and higher background, achieving a slope of ~0.56 (Fig. 5f); nevertheless, the correlation coefficient was superb (~0.98) indicating that while the phone detected roughly half the positives, it enabled accurate quantitation of the sample (Fig. 5g). Based on RT-ddPCR measurements made using commercially available Bio-Rad kits, we measured a limit of detection of 1 copy per μL (1000 copies per mL) with 20/20 using contrived RNA samples. Below this we detected 17/20 for 1 copy per 5 μL. At this concentration, Poisson statistics predicts only 12/20 samples will contain one or more viral copies such that, by increasing total analyzed sample volume, the LOD may be reduced. Conversely Poisson statistics predicts 8/20 will have no copies per 5 μL. This demonstrates the feasibility of our assay for POC viral load measurements.

Discussion

We have described a simple, microfluidic-free workflow for viral load quantitation. Our approach matches the accuracy of gold standard qPCR and uses a smartphone as the readout. We show through the analysis of over 100 patient samples the ability to quantitate viral load over 3 orders of

magnitude. While our results demonstrate the feasibility of simple, accurate viral load quantitation in the POC, the current prototype is not ready for broad use, since it relies on hand shaking to generate droplets and manual transfer of sample to the imaging chamber. Both steps can vary between users and, thus, would need to be automated for use by non-experts. Automated and more controlled emulsification can be achieved through homogenization, vortexing, and bulk shearing, with the added benefit of potentially yielding smaller, more uniform droplets that will increase accuracy. Emulsification can also be achieved with microfluidics since it generates monodispersed droplets that simplify quantitation.[26] Further microfluidic optimization of the chip design can also support sample preparation within the viewing chamber further minimizing user interactions.[27] However, we have shown here that polydispersed emulsions can also enable accurate digital molecular counting, with the added benefit of being simpler to generate.[28] The need to transfer samples can be avoided by integrating the imaging chamber into the sample holder. Several commercial devices that use low cost and passive fluidic techniques have been demonstrated to enable this.[29]

In addition to providing accurate viral load measurements, droplet compartmentalization has other useful features. Due to its ability to sequester inhibitors in droplet subsets and run reactions to saturation, droplet reactions are more robust to inhibition, which is important for POC settings in which sample pre-processing is difficult. Additionally, droplet methods are compatible with fluorescence multiplexing to simultaneously quantitate several targets, or to determine co-occurrence of subsequences within a single target molecule. This can be used to screen for multiple viruses or variants of the same virus (*e.g.*, SARS-CoV-2 variants) in a single test or to determine viral intactness and viability with primers targeting different locations on each virus to estimate patient infectiousness.[30,31] While we have focused on SARS-CoV2, our sddRT-LAMP reaction can be targeted to any nucleic acid to which primers can be designed, including from other viruses or microorganisms, which is relevant to sepsis and pulmonary, gastrointestinal, and urinary tract infections.

Materials and methods

sddRT-LAMP, RT-ddPCR, and RT-qPCR protocol

sddRT-LAMP reactions were compared to RT-ddPCR and RT-qPCR. A LAMP master mix is prepared with 1× isothermal amplification buffer (NEB B0537S), 7.5 mM $MgSO_4$ (NEB B1003S), 1.875 mM dNTPs (ThermoFisher Scientific R1122), 8 U Bst 2.0 WarmStart DNA polymerase (NEB M0538L), 100 U SuperScript III reverse transcriptase (ThermoFisher Scientific 18 080 093) and the LAMP primer set, which consists of 3.4 μM FIP (IDT, GTGCAATTTGCGGCCAATGTTTGTTTTTCAAGGA AATTTTGGGGACCAG), 3.4 μM BIP-FAM (IDT, /56-FAM/CCAG CGCTTCAGCGTTCTTCTTTTTCAACCACGTTCCCGAAGG), 5.1 μM BIP*-BHQ1 (IDT, CTGAAGCGCTGG/3BHQ_1/), 1.7 μM LB (IDT, AATGTCGCGCATTGGCATGG), 1.7 μM LF (IDT, CAGTTC CTTGTCTGATTAGTTC), 0.4 μM F3 (IDT, CTGCCACTAAAGCA TACAATGT), and 0.4 μM B3 (IDT, TTGATGGCACCTGTGTAG G). A qPCR master mix is prepared using the Luna SARS-CoV-2 RT-qPCR multiplex assay kit (NEB E3019L) according to manufacturer guidelines. The ddPCR master mix is prepared with the One-Step RT-ddPCR Advanced Kit for Probes (Bio-Rad, 1 864 021) with COVID N primers (Bio-Rad, dEXD54243734) according to manufacturer guidelines. The following reagent was deposited by the Centers for Disease Control and Prevention and obtained through BEI Resources, NIAID, NIH: SARS-Related Coronavirus 2, Isolate USA-WA1/2020, Heat Inactivated, NR-52286. For the characterization of sddRT-LAMP, a dilution series of this inactivated SARS-COV-2 intact virus is prepared at 1/200 (2680 copies per μL), 1/2000 (268 copies per μL), 1/20 000 (26.8 copies per μL), and 1/200 000 (2.68 copies/μL) dilutions. Lysis is performed on ice over 5 minutes after adding 10 μL of QuickExtract RNA (Lucigen Corporation, QER090150) to 90 μL of each dilution. For sddRT-LAMP, 15 μL of sddRT-LAMP master mix is added to 5 μL of each dilution in triplicate and mixed by agitation *via* flicking. Emulsification is performed by adding 40 μL of 2% (w/v) 008-Fluorosurfactant (Ran Biotechnologies) in Novec-7500 Engineering Fluid (3 M, 98–0212–2928-5) to each sample, then agitating by shaking for 30 seconds until no droplets were visible by eye and the emulsion is opaque. Each sample is checked to ensure complete emulsification of the entire sample then thermocycled at 55 °C for 10 min, 65 °C for 30 min, then 25 °C for 5 min. The entire sample is then loaded into the imaging chamber for imaging using an EVOS FL Auto (Life Technologies) with a single layer chip allowing for quantification of positive droplet and polydispersity. For qPCR, 15 μL of the qPCR master mix is added to 5 μL of each dilution in triplicate and thermocycled according to 25 °C for 30 s, 55 °C for 10 min, 95 °C for 1 min, then 45 cycles of 95 °C for 10 s and 60 °C for 30 seconds with plate read. For RT-ddPCR, 15 μL of the RT-ddPCR master mix is added to 5 μL of each dilution in triplicate. The samples were then run on the QX200 Droplet Generator (Bio-Rad) according to manufacturer guidelines and thermocycled according to 50 °C for 60 min, 95 °C for 10 min, then 40 cycles of 94 °C for 30 s and 55 °C for 60 s, followed by 98 °C for 10 min and 4 °C for 30 min. The resulting droplets were then run on the QX200 Droplet Reader (Bio-Rad) allowing for quantification of positive droplets.

Fabrication of dual-height imaging chamber and assembly of iPhone-based fluorescent microscope

Standard photolithography is used to make two-layered structures (80 and 190 μm, respectively) on a 3 inch silicon wafer with SU-8 3025 photoresist (MicroChem, Westborough, MA, USA). PDMS prepolymer and curing agent (Sylgard 184 silicone elastomer kit) is mixed at a ratio 1 : 10, de-gassed in a vacuum chamber, poured over the mold, de-gassed until no more bubbles were visible and baked at 65 °C overnight. The

PDMS replica is removed from the mold, inlets, and outlets punched with a custom made 3 mm biopsy punch and individually plasma bonded to glass slides (75 × 25 × 1 mm, Fisher Scientific) by treating with oxygen plasma for 45 s at 1 mbar (PDC-001, Harrick Plasma). The device is baked at 65 °C overnight and treated with Aquapel (PPG Industries) with a contact time of about 1 minute and purged with HFE 7500 oil (3 M™ Novec™ 7500 Engineered Fluid). The bottom of the glass slide is covered with a black vinyl tape-based mask, with approximately 12 mm circular opening in the middle for the circular 2-d chamber (also known as the observation chamber), to limit the amount of light penetrating the PDMS chip. We used a hollow steel punch (12 mm, 1/2 inch, General, No. 1280) to make the circular opening in the black vinyl tape. The black vinyl tape-based mask is covered with a double-sided adhesive tape from Intertape Polymer Group, which is punched with a hollow steel puncher (19 mm, 3/4-inch, General, No. 1280) to create a 19 mm circular opening that would allow imaging of the whole surface area of the observation chamber. The other side of double-sided adhesive tape is used to attach the chip to the iPhone-based fluorescent microscope during sample imaging. A 470 nm excitation gel filter (25 × 35 mm Lee Filters, Deep Purple #797) is attached to the side of the PDMS chip closer to the shallower part of the 2-d chamber (80 μm in depth).

The iPhone-based fluorescent microscope consists of the iPhone itself, 10× lens, bandpass filter, fluorescent light source, and battery powersource. Briefly, the WF10X 18 mm lens (Semrock, #FF01-524/24-25) and 524/24 nm bandpass filter is affixed to the iPhone 8+ (Apple, A1897) with a lens holder (LUXUN, B08KGDQ8BS). The fluorescent light source consists of two 470 nm LEDs positioned at 45° angels facing the corner of the PDMS element, which are powered by two 3 V coin batteries affixed to the lens holder.

Isothermal sddRT-LAMP protocol

The evaluation of patient samples is performed using an isothermal sddRT-LAMP protocol. In brief, a sddRT-LAMP master mix consisting of 1× isothermal amplification buffer (NEB B0537S), 7.5 mM $MgSO_4$ (NEB B1003S), 1.875 mM dNTPs (ThermoFisher Scientific R1122), 8 U Bst 2.0 WarmStart DNA polymerase (NEB M0538L), 7.5 U WarmStart RTx reverse transcriptase (NEB, M0380S) and the LAMP primer set is prepared. To lyse the sample, 80 μL of patient samples collected at UCSF Clinical Microbiology Laboratory is combined with 20 μL of QuickExtract RNA (Lucigen Corporation, QER090150) and mixed by pipetting before incubating at 95 °C for 3 min. After lysis, 40 μL of the sddRT-LAMP master mix is mixed 10 μL of the lysed sample before adding 65 μL of 2% (w/v) 008-Fluorosurfactant (Ran Biotechnologies) in Novec-7500 Engineering Fluid (3 M, 98-0212-2928-5). Emulsification is performed by shaking for 30 s to emulsify until opaque and ensuring no droplets were visible by eye. Afterwards, the emulsion is incubated at 65 °C for 30 min then 20 °C for 5 min. For imaging, the entire emulsion is pipetted into a multi-layered device and then imaged on either the custom-built iPhone-based fluorescent microscope or an EVOS FL Auto (Life Technologies).

Conflicts of interest

There are no conflicts to declare.

Acknowledgements

We would like to thank Sarah Pyle and Cyrus Modavi for the illustrations. The work developing this protocol was supported by the NHLBI (U54HL119893), National Institutes of Health (R01-EB019453-02 and U01-AI129206-01), the Chan-Zuckerberg Biohub Investigator Program, Defense Advanced Research Projects Agency (DARPA) under Contract No. W911NF1920013, and Virology Surveillance and Diagnosis Branch, Influenza Division, Centers for Disease Control and Prevention, under BAA 75D30-11-9C-06818 (CDC3). The content of the information does not necessarily reflect the position or the policy of the Government, and no official endorsement should be inferred.

References

1 M. Valentine-Graves, E. Hall, J. Guest, E. Adam, R. Valencia, I. Hardee, K. Shinn, T. Sanchez, A. J. Siegler and P. Sullivan, At-Home Self-Collection of Saliva, Oropharyngeal Swabs and Dried Blood Spots for SARS-CoV-2 Diagnosis and Serology: Post-Collection Acceptability of Specimen Collection Process and Patient Confidence in Specimens, *PLoS One*, 2020, **15**(8), e0236775, DOI: **10.1371/journal.pone.0236775**.

2 C. Herbert, J. Broach, W. Heetderks, F. Qashu, L. Gibson, C. Pretz, K. Woods, V. Kheterpal, T. Suvarna, C. Nowak, P. Lazar, D. Ayturk, B. Barton, C. Achenbach, R. Murphy, D. McManus and A. Soni, Feasibility of At-Home Serial Testing Using Over-the-Counter SARS-CoV-2 Tests With a Digital Smartphone App for Assistance: Longitudinal Cohort Study, *JMIR Form. Res.*, 2022, **6**(10), e35426, DOI: **10.2196/35426**.

3 I. J. B. Møller, A. R. Utke, U. K. Rysgaard, L. J. Østergaard and S. Jespersen, Diagnostic Performance, User Acceptability, and Safety of Unsupervised SARS-CoV-2 Rapid Antigen-Detecting Tests Performed at Home, *Int. J. Infect. Dis.*, 2022, **116**, 358–364, DOI: **10.1016/j.ijid.2022.01.019**.

4 J. H. Kotnik, S. Cooper, S. Smedinghoff, P. Gade, K. Scherer, M. Maier, J. Juusola, E. Ramirez, P. Naraghi-Arani, V. Lyon, B. Lutz and M. Thompson, Flu@home: The Comparative Accuracy of an At-Home Influenza Rapid Diagnostic Test Using a Prepositioned Test Kit, Mobile App, Mail-in Reference Sample, and Symptom-Based Testing Trigger, *J. Clin. Microbiol.*, 2022, **60**(3), e0207021, DOI: **10.1128/jcm.02070-21**.

5 N. Engel and N. Pant Pai, Qualitative Research on Point-of-Care Testing Strategies and Programs for HIV, *Expert Rev. Mol. Diagn.*, 2015, **15**(1), 71–75, DOI: **10.1586/14737159.2015.960518**.

6 A. Bektaş, M. F. Covington, G. Aidelberg, A. Arce, T. Matute, I. Núñez, J. Walsh, D. Boutboul, C. Delaugerre, A. B. Lindner, F. Federici and A. D. Jayaprakash, Accessible LAMP-Enabled Rapid Test (ALERT) for Detecting SARS-CoV-2, *Viruses*, 2021, **13**(5), 742, DOI: **10.3390/v13050742**.

7 M. W. McCarthy, At-Home Coronavirus Testing: The next Game-Changer?, *Expert Rev. Mol. Diagn.*, 2021, **21**(1), 1–2, DOI: **10.1080/14737159.2021.1873133**.

8 A. Harmon, C. Chang, N. Salcedo, B. Sena, B. B. Herrera, I. Bosch and L. E. Holberger, Validation of an At-Home Direct Antigen Rapid Test for COVID-19, *JAMA Netw. Open*, 2021, **4**(8), e2126931, DOI: **10.1001/jamanetworkopen.2021.26931**.

9 G. C. Mak, S. S. Lau, K. K. Wong, N. L. Chow, C. Lau, E. T. Lam, R. C. Chan and D. N. Tsang, Analytical Sensitivity and Clinical Sensitivity of the Three Rapid Antigen Detection Kits for Detection of SARS-CoV-2 Virus, *J. Clin. Virol.*, 2020, **133**, 104684, DOI: **10.1016/j.jcv.2020.104684**.

10 H. Scheiblauer, A. Filomena, A. Nitsche, A. Puyskens, V. M. Corman, C. Drosten, K. Zwirglmaier, C. Lange, P. Emmerich, M. Müller, O. Knauer and C. M. Nübling, Comparative Sensitivity Evaluation for 122 CE-Marked Rapid Diagnostic Tests for SARS-CoV-2 Antigen, *Eurosurveillance*, 2022, **27**(3), 2100441, DOI: **10.2807/1560-7917.ES.2021.26.44.2100441**.

11 K. I. Aronson, R. O'Beirne, F. J. Martinez and M. M. Safford, Barriers to Antigen Detection and Avoidance in Chronic Hypersensitivity Pneumonitis in the United States, *Respir. Res.*, 2021, **22**(1), 225, DOI: **10.1186/s12931-021-01817-6**.

12 R. Pu, S. Liu, X. Ren, D. Shi, Y. Ba, Y. Huo, W. Zhang, L. Ma, Y. Liu, Y. Yang and N. Cheng, The Screening Value of RT-LAMP and RT-PCR in the Diagnosis of COVID-19: Systematic Review and Meta-Analysis, *J. Virol. Methods*, 2022, **300**, 114392, DOI: **10.1016/j.jviromet.2021.114392**.

13 Y. Tanimoto, A. Mori, S. Miyamoto, E. Ito, K. Arikawa and T. Iwamoto, Comparison of RT-PCR, RT-LAMP, and Antigen Quantification Assays for the Detection of SARS-CoV-2, *Jpn. J. Infect. Dis.*, 2022, **75**(3), 249–253, DOI: **10.7883/yoken.JJID.2021.476**.

14 K. Minami, R. Masutani, Y. Suzuki, M. Kubota, N. Osaka, T. Nakanishi, T. Nakano and A. Ukimura, Evaluation of SARS-CoV-2 RNA Quantification by RT-LAMP Compared to RT-QPCR, *J. Infect. Chemother.*, 2021, **27**(7), 1068–1071, DOI: **10.1016/j.jiac.2021.05.004**.

15 M. Cevik, M. Tate, O. Lloyd, A. E. Maraolo, J. Schafers and A. Ho, SARS-CoV-2, SARS-CoV, and MERS-CoV Viral Load Dynamics, Duration of Viral Shedding, and Infectiousness: A Systematic Review and Meta-Analysis, *Lancet Microbe*, 2021, **2**(1), e13–e22, DOI: **10.1016/S2666-5247(20)30172-5**.

16 M. Riediker, L. Briceno-Ayala, G. Ichihara, D. Albani, D. Poffet, D.-H. Tsai, S. Iff and C. Monn, Higher Viral Load and Infectivity Increase Risk of Aerosol Transmission for Delta and Omicron Variants of SARS-CoV-2, *Swiss Med. Wkly.*, 2022, **152**(0102), w30133, DOI: **10.4414/SMW.2022.w30133**.

17 A. Baer and K. Kehn-Hall, Viral Concentration Determination Through Plaque Assays: Using Traditional and Novel Overlay Systems, *J. Visualized Exp.*, 2014, (93), 52065, DOI: **10.3791/52065**.

18 L. A. Pereira, B. A. Lapinscki, M. C. Debur, J. S. Santos, R. R. Petterle, M. B. Nogueira, L. R. R. Vidal, S. M. De Almeida and S. M. Raboni, Standardization of a High-Performance RT-QPCR for Viral Load Absolute Quantification of Influenza A, *J. Virol. Methods*, 2022, **301**, 114439, DOI: **10.1016/j.jviromet.2021.114439**.

19 J. B. Case, A. L. Bailey, A. S. Kim, R. E. Chen and M. S. Diamond, Growth, Detection, Quantification, and Inactivation of SARS-CoV-2, *Virology*, 2020, **548**, 39–48, DOI: **10.1016/j.virol.2020.05.015**.

20 A. Forootan, R. Sjöback, J. Björkman, B. Sjögreen, L. Linz and M. Kubista, Methods to Determine Limit of Detection and Limit of Quantification in Quantitative Real-Time PCR (QPCR), *Biomol. Detect. Quantif.*, 2017, **12**, 1–6, DOI: **10.1016/j.bdq.2017.04.001**.

21 D. Pillay, HIV Viral Load: The Myth of the Undetectable?, *Rev. Med. Virol.*, 2002, **12**(6), 391–396, DOI: **10.1002/rmv.373**.

22 C. Mio, A. Cifù, S. Marzinotto, B. Marcon, C. Pipan, G. Damante and F. Curcio, Validation of a One-Step Reverse Transcription-Droplet Digital PCR (RT-DdPCR) Approach to Detect and Quantify SARS-CoV-2 RNA in Nasopharyngeal Swabs, *Dis. Markers*, 2021, **2021**, 1–6, DOI: **10.1155/2021/8890221**.

23 C. M. Hindson, J. R. Chevillet, H. A. Briggs, E. N. Gallichotte, I. K. Ruf, B. J. Hindson, R. L. Vessella and M. Tewari, Absolute Quantification by Droplet Digital PCR versus Analog Real-Time PCR, *Nat. Methods*, 2013, **10**(10), 1003–1005, DOI: **10.1038/nmeth.2633**.

24 A. A. Kojabad, M. Farzanehpour, H. E. G. Galeh, R. Dorostkar, A. Jafarpour, M. Bolandian and M. M. Nodooshan, Droplet Digital PCR of Viral DNA/RNA, Current Progress, Challenges, and Future Perspectives, *J. Med. Virol.*, 2021, **93**(7), 4182–4197, DOI: **10.1002/jmv.26846**.

25 N. N. Kinloch, G. Ritchie, W. Dong, K. D. Cobarrubias, H. Sudderuddin, T. Lawson, N. Matic, J. S. G. Montaner, V. Leung, M. G. Romney, C. F. Lowe, C. J. Brumme and Z. L. Brumme, SARS-CoV-2 RNA Quantification Using Droplet Digital RT-PCR, *J. Mol. Diagn.*, 2021, **23**(8), 907–919, DOI: **10.1016/j.jmoldx.2021.04.014**.

26 Z. Zhu, G. Jenkins, W. Zhang, M. Zhang, Z. Guan and C. J. Yang, Single-Molecule Emulsion PCR in Microfluidic Droplets, *Anal. Bioanal. Chem.*, 2012, **403**(8), 2127–2143, DOI: **10.1007/s00216-012-5914-x**.

27 C. Liu, E. Geva, M. Mauk, X. Qiu, W. R. Abrams, D. Malamud, K. Curtis, S. M. Owen and H. H. Bau, An Isothermal Amplification Reactor with an Integrated Isolation Membrane for Point-of-Care Detection of Infectious Diseases, *Analyst*, 2011, **136**(10), 2069, DOI: **10.1039/c1an00007a**.

28 S. A. Byrnes, T. C. Chang, T. Huynh, A. Astashkina, B. H. Weigl and K. P. Nichols, Simple Polydisperse Droplet Emulsion Polymerase Chain Reaction with Statistical Volumetric Correction Compared with Microfluidic Droplet Digital Polymerase Chain Reaction, *Anal. Chem.*, 2018, **90**(15), 9374–9380, DOI: **10.1021/acs.analchem.8b01988**.

29 F. Cui, M. Rhee, A. Singh and A. Tripathi, Microfluidic Sample Preparation for Medical Diagnostics, *Annu. Rev.*

Biomed. Eng., 2015, **17**(1), 267–286, DOI: **10.1146/annurev-bioeng-071114-040538**.

30 S. T. Lance, D. J. Sukovich, K. M. Stedman and A. R. Abate, Peering below the Diffraction Limit: Robust and Specific Sorting of Viruses with Flow Cytometry, *Virol. J.*, 2016, **13**(1), 201, DOI: **10.1186/s12985-016-0655-7**.

31 K. M. Bruner, Z. Wang, F. R. Simonetti, A. M. Bender, K. J. Kwon, S. Sengupta, E. J. Fray, S. A. Beg, A. A. R. Antar, K. M. Jenike, L. N. Bertagnolli, A. A. Capoferri, J. T. Kufera, A. Timmons, C. Nobles, J. Gregg, N. Wada, Y.-C. Ho, H. Zhang, J. B. Margolick, J. N. Blankson, S. G. Deeks, F. D. Bushman, J. D. Siliciano, G. M. Laird and R. F. Siliciano, A Quantitative Approach for Measuring the Reservoir of Latent HIV-1 Proviruses, *Nature*, 2019, **566**(7742), 120–125, DOI: **10.1038/s41586-019-0898-8**.